Organic & Biomolecular Chemistry

Cite this: *Org. Biomol. Chem.*, 2012, **10**, 7372

www.rsc.org/obc

PAPER

Investigating the oxidation of alkenes by non-heme iron enzyme mimics†

Sarah M. Barry,‡[a] Helge Mueller-Bunz[b] and Peter J. Rutledge*[a]

Received 1st May 2012, Accepted 29th June 2012
DOI: 10.1039/c2ob25834j

Iron is emerging as a key player in the search for efficient and environmentally benign methods for the functionalisation of C–H bonds. Non-heme iron enzymes catalyse a diverse array of oxidative chemistry in nature, and small-molecule complexes designed to mimic the non-heme iron active site have great potential as C–H activation catalysts. Herein we report the synthesis of a series of organic ligands that incorporate key features of the non-heme iron active site. Iron(II) complexes of these ligands have been generated *in situ* and their ability to promote hydrocarbon oxidation has been investigated. Several of these systems promote the biomimetic dihydroxylation of cyclohexene at low levels, when hydrogen peroxide is used as the oxidant; allylic oxidation products are also observed. An investigation of ligand stability reveals formation of several breakdown products under the conditions of the oxidative turnover reactions. These products arise *via* oxidative decarboxylation, dehydration and deamination reactions. Taken together these results indicate that competing mechanisms are at play with these systems: biomimetic hydroxylation involving high-valent iron species, and allylic oxidation *via* Fenton chemistry and Haber–Weiss radical pathways.

Introduction

Chemists have long looked to nature for inspiration in the design of new oxidation catalysts.[1–8] Non-heme iron enzymes catalyse a diverse range of oxidation reactions in biology, including desaturation and cyclisation (oxidase activity), hydroxylation and epoxidation (mono-oxygenase activity), dihydroxylation, and oxidative ring opening reactions (di-oxygenase activity).[5–14]

Over the past decade, significant information has been garnered concerning the structure and catalytic mechanism of non-heme iron enzymes.[5–8] X-Ray crystal structures reveal a conserved active site which incorporates an iron(II) centre bound by three protein-derived ligands, two histidines and one carboxylate, occupying one face of the iron(II) coordination sphere (Fig. 1).[15,16] While this '2-His-1-carboxylate' triad has emerged as a common motif across the family, non-heme iron enzymes utilise a range of different cofactors and mechanisms to drive reductive cleavage of the O–O bond.[5,6,17] In cleaving this bond, non-heme iron oxidases generate high-valent iron-oxo intermediates (iron(IV)- or iron(V)-oxo), now generally accepted as the active oxidising species in these systems.[18–20] Such species have been spectroscopically characterized in several non-heme iron enzymes, including taurine/α-ketoglutarate dioxygenase (TauD),[21] prolyl-4-hydroxylase[22] and tyrosine hydroxylase.[23]

Further mechanistic insight has been derived using small-molecule active site models of non-heme iron catalysis.[5–8] The most effective of these biomimetic systems are based upon neutral, multidentate ligands such as tris(2-pyridylmethyl)amine (TPA),[24] bispidines,[25] chiral bis-pyrrolidines (PDP or BPBP),[26–28] and tetramethylguanidines (TMG_3tren and TMG_2dien).[29,30] When complexed with iron(II) and combined with a suitable oxidant (*e.g.* hydrogen peroxide, *tert*-butylhydroperoxide or molecular oxygen), these mimics can carry out stereoselective dihydroxylation, epoxidation and hydroxylation reactions on a range of hydrocarbon substrates, with good to excellent catalytic efficiency. Model complexes have also been used to generate high-valent iron-oxo intermediates similar to those proposed to mediate non-heme catalytic pathways *in vivo*, allowing visualization of oxygen activation in model systems by isolating and characterising iron(III)-hydroperoxo and iron(IV)-oxo intermediates,[31–36] and recently an iron(V) species.[37]

Towards the goal of constructing small-molecule iron-based catalysts for hydrocarbon oxidation, we have recently reported a range of ligands **2–4** designed to mimic the non-heme iron active site (Fig. 1).[38–41] These ligands combine with iron(II)

[a]*School of Chemistry F11, The University of Sydney, NSW 2006, Australia. E-mail: peter.rutledge@sydney.edu.au; Fax: +61 2 9351 3329; Tel: +61 2 9351 5020*
[b]*School of Chemistry and Chemical Biology, University College Dublin, Belfield, Dublin 4, Ireland*

†Electronic supplementary information (ESI) available. CCDC 879768 and 879769. For ESI and crystallographic data in CIF or other electronic format see DOI: 10.1039/c2ob25834j

‡Current address: Department of Chemistry, University of Warwick, Coventry, CV4 7AL, UK.

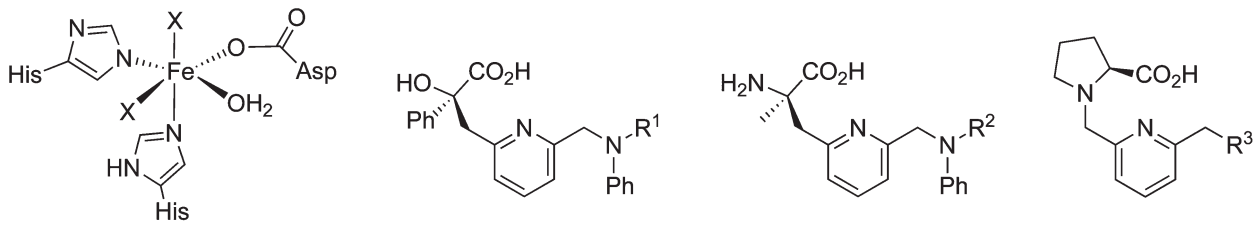

Fig. 1 Generalized non-heme iron active site **1**, and ligand architectures **2–4** previously constructed to mimic its structure and function (R^1 = Et, allyl; R^2 = Ph; R^3 = -1-(pyrrolidine-2-carboxylic acid), -OH or -((*S*)-1-phenylethyl)amino; X = solvent or substrate-derived ligand).[38–41]

acetate and hydrogen peroxide in methanol solvent to convert a range of simple alkenes (C_5–C_8, cyclic and straight-chain) to diols and allylic oxidation products.[39,41]

To better understand and thus expand the catalytic behaviour of these ligands, we now report a detailed investigation of the factors that influence activity in ligands of general structure **2** and the related ligands **5–7**, which incorporate different elements of the larger structure **2** (Fig. 2).

Ligands **2** are designed so that the pyridine and tertiary amine ligands model the histidine residues of the non-heme iron active site, mandelic acid mimics the carboxylate and water ligands of the natural system; the R group of the exocyclic amine is varied by incorporating different aniline derivatives. This design has been developed considering the propensity of iron(II) complexes to undergo competing intermolecular oxidation reactions to give bridged products such as Fe(III)–O–Fe(III) species. Thus two pendant phenyl groups are included in the structure to increase steric bulk and inhibit such intermolecular interactions that would render the complex inactive. Ligands **2a–d** are tetradentate and designed to form iron(II) complexes in which there are two vacant coordination sites for peroxide binding, while also providing steric bulk around the metal centre. This arrangement of vacant *cis* positions mimics the naphthalene dioxygenase active site,[42] and is in accordance with the accepted thesis that two vacant sites *cis* to each other are absolutely required for a small-molecule iron complex to effect dihydroxylation using hydrogen peroxide as oxidant.[24] Ligands **5**, **6** and **7** represent the 'component parts' of the larger ligand **2**, and have been studied to investigate the influence of each part on reactivity.

Results and discussion

Synthesis of ligands 2a–d

Ligands **2a–d** were prepared from (*S*)-mandelic acid **7**, pyridine-2,6-dimethanol **8**, and *N*-substituted anilines **9a–d** (Scheme 1), extending our previously reported synthesis of ligand **2b**.[38,39]

Diol **8** was desymmetrised and converted to key bromide intermediate **11** in five steps as reported previously.[38] The stereochemistry of the starting mandelic acid is preserved throughout this sequence by employing the dioxolanone as both protecting group and chiral auxiliary,[43] which ultimately delivers ligands **2a–d** in enantiomerically pure form. An X-ray crystal structure† of **11** was solved (Fig. 3), confirming that the stereochemical integrity is preserved through the alkylation–deprotection–bromination sequence, and that both stereocentres have the stereochemistry expected.

Coupling of bromide **11** with the *N*-substituted anilines **9a–d** gives protected ligands **12a–d**. *N*-Methylaniline **9a**, *N*-ethylaniline **9b** and diphenylamine **9d** are commercially available, *N*-*tert*-butylaniline was made from *N*-*tert*-butylamine and bromobenzene following a literature procedure.[45]

Optimisation studies with the ethyl analogue **9b** revealed that using sodium hydride as base in DMF solvent returned no reaction, while reactions with *n*-BuLi in THF were low-yielding unless *N*,*N*′-dimethylpropyleneurea (DMPU) was included as co-solvent.[46] The amine is efficiently deprotonated at 0 °C in all cases, but the optimum temperature for the coupling step varies with the amine being coupled: −78 °C for **9a**, −40 °C with **9b**, −5 °C for **9c** and −15 °C for **9d** (Scheme 1). Using these optimised conditions good yields were achieved for the methyl

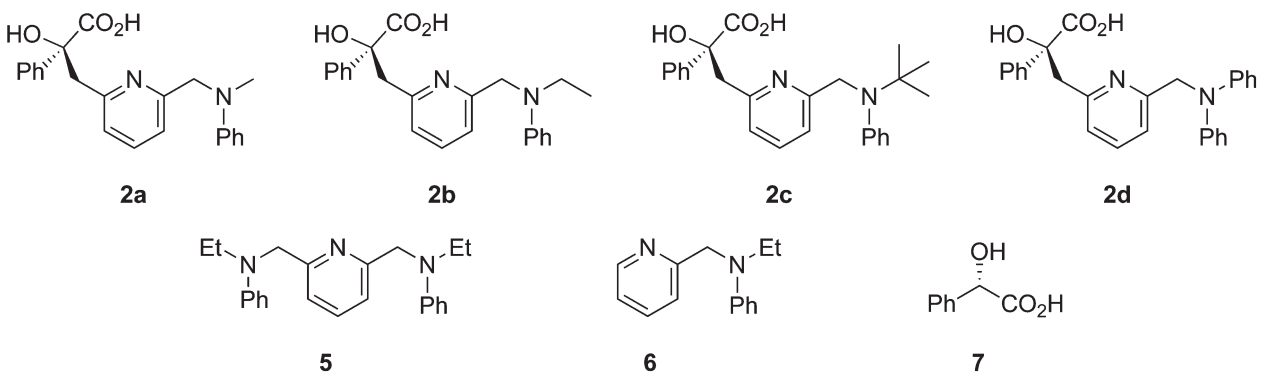

Fig. 2 Ligands used in this study.

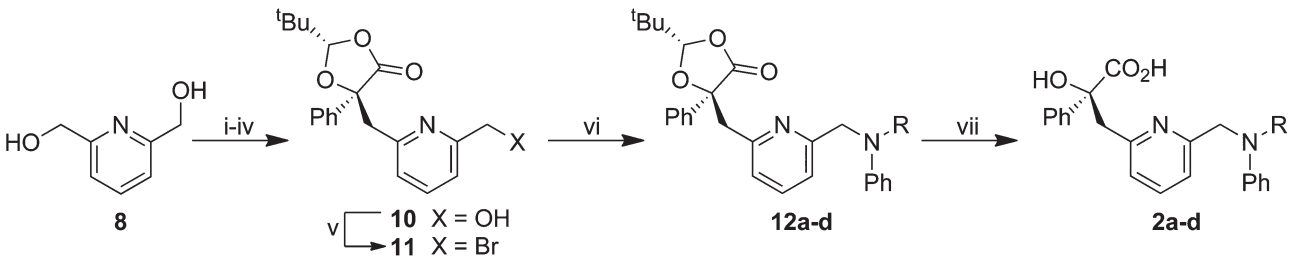

Scheme 1 Synthesis of ligands **2a–d**; i. NaH, TBDMSCl, DCM, rt, 5 hours, 57%; ii. CBr_4, PPh_3, DCM, rt, 2 hours, 94%; iii. ((2*S*,4*S*)-2-(*tert*-butyl)-5-oxo-4-phenyl-1,3-dioxolan-4-yl)lithium, THF, −78 °C, 6 hours, 91%; iv. TBAF, THF, rt, 90 minutes, 88%; v. CBr_4, PPh_3, DCM, rt, 2 hours, 77%; vi. a. *n*-BuLi–DMPU, MeNHPh **9a**, THF, −78 °C, 5 hours, 84%; *or* b. *n*-BuLi–DMPU, EtNHPh **9b**, THF, −40 °C, 5 hours, 85%; *or* c. *n*-BuLi–DMPU, *t*BuNHPh **9c**, THF, −5 °C, 5 hours, 40%; *or* d. *n*-BuLi, $HNPh_2$ **9d**, THF, −15 °C, 4 hours, 82%; vii. a.–c. 1 M LiOH, THF, reflux, 17 hours then 1 M HCl; *or* d. 1 M LiOH, MeOH, reflux, 17 hours then 1 M HCl (91–95%).

(**12a**, 84%), ethyl (**12b**, 85%) and phenyl (**12d**, 82%) analogues, but the more hindered *tert*-butyl derivative **12c** was less cooperative and returned a lower yield (40%) despite efforts to further optimise this reaction, presumably a result of steric effects.

The diphenyl compound **12d** was isolated as a white crystalline solid after column chromatography and an X-ray crystal structure† of **12d** was solved (Fig. 4). This structure confirms the *cis* relationship of the *tert*-butyl and phenyl substituents on the dioxolanone ring, and that this five-membered ring sits over the top of the pyridine nitrogen in the crystalline compound.

Deprotection of **12a–d** proceeded smoothly in all cases and gave excellent yields. The hydrolysis reaction was carried out in aqueous base (1 M lithium hydroxide) and a minimum of organic co-solvent. THF was used for **12a–c**, however **12d** showed no reaction in water–THF even at reflux due to phase separation, so water–methanol was used instead. The crude lithium salt of the ligand is protonated during workup to give the neutral product, which was separated from the lithium chloride side product by triturating with DCM or chloroform.

Synthesis of ligands 5 and 6

To make the triamine ligand **5**, pyridine-2,6-dimethanol **8** was first converted to the dibromide, using triphenylphosphine and tetrabromomethane as in our synthesis of mono-bromide **11**.[38] Then *N*-ethylaniline **9b** was introduced using the same method as for preparation of **12b** to give **5** as a flakey crystalline solid in reasonable yield (55%) over the two steps (Scheme 2a).

Accessing bidentate ligand **6** required a change in strategy, as derivatives of pyridine-2-methanol **13** that bear pendant leaving groups are prone to dimerise, forming pyrazinium salts.[41,47,48] Thus attempts to brominate **13** using the same mild, neutral conditions described above for alcohol **8** gave 6,12-dihydrodipyrido-[1,2-*a*:1′,2′-*d*]pyrazine-5,11-diium dibromide as a crystalline solid (data not shown), while the tosylate derivative of **13** decomposed to elimination products. These problems are avoided by keeping the pyridine nitrogen protonated: treating pyridine-2-methanol **13** with neat thionyl chloride as reported by Winterfield and Flick affords 2-chloromethylpyridine as its hydrochloride salt in excellent yield (93%).[49] This salt is highly hygroscopic and thus difficult to handle which compromises the yield of the following, moisture-sensitive step. Nonetheless reaction with the combination of *n*-BuLi and *N*-ethylaniline completed the synthesis of ligand **6** in 37% yield over the two steps. (Note that *N*-ethylaniline was combined with two equivalents of *n*-BuLi to account for the hydrochloride salt, however the base was not added directly to 2-chloromethylpyridine hydrochloride before the nucleophile to avoid pyrazinium formation.)

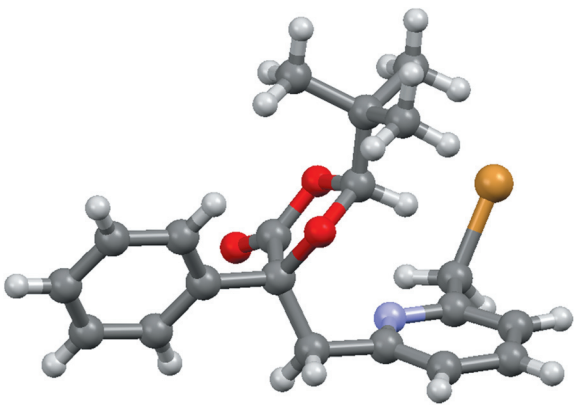

Fig. 3 X-Ray crystal structure of bromide **11**, synthesised according to the procedure we have reported previously[38] and crystallised by slow evaporation of a cyclohexane–ether solution; image generated using Mercury CSD 2.0.[44]

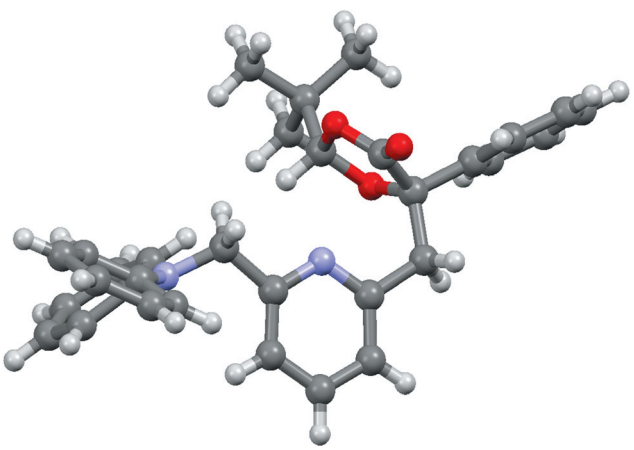

Fig. 4 X-Ray crystal structure of diphenylamine derivative **12d**; image generated using Mercury CSD 2.0.[44]

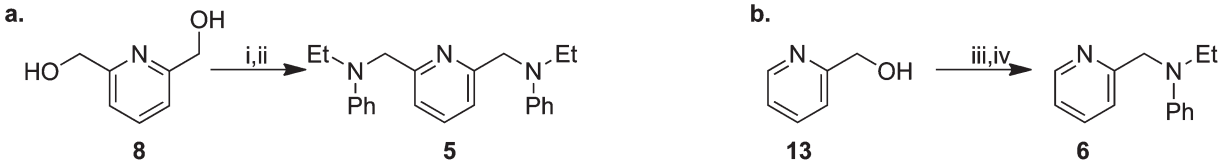

Scheme 2 Synthesis of ligands **5** and **6**; i. CBr_4, PPh_3, DCM, rt, 16 hours, 75%; ii. *n*-BuLi–DMPU, EtNHPh (2 eq), THF, −40 °C, 5 hours, 73%; iii. $SOCl_2$, reflux, 16 hours, 93%; iv. *n*-BuLi, HNPhEt, THF–DMPU, −41 °C, 40%.

It is interesting to note that bromide **11** does not undergo dimerization to a pyrazinium derivative: it is a white, crystalline solid that does not show any sign of degradation even after standing for several months at room temperature. This is presumably a steric effect, and the X-ray crystal structure of **11** (Fig. 3) shows clearly that the pyridine nitrogen is effectively shielded by the bulk of the dioxolanone ring, which also appears to hinder access to σ* of the C–Br bond.

Oxidative turnover reactions

The combination of iron(II), a ligand and hydrogen peroxide can give rise to a variety of different oxidation products from an alkene substrate (Scheme 3). Biomimetic dihydroxylation (Path A) promoted by an iron-ligand complex can convert cyclohexene **14** to the *cis*-diol **15** using a high-valent iron-oxo intermediate.[31–33] Competing reactions *via* radical mechanisms (Path B) traditionally associated with Fenton and Haber–Weiss pathways leads to the allylic oxidation products alcohol **16** and ketone **17**.[50] The hydroperoxide **18** (a potential precursor of both **16** and **17**) may also be formed *via* the radical path and isolated under some circumstances, and the epoxide **19** can arise from reaction of **18** with another molecule of the alkene **14**.[6,16]

Iron complexes of ligands **2a–d** and **5–7** were formed *in situ* by mixing the sodium salt of the ligand with an equimolar amount of an iron(II) salt in degassed methanol at room temperature. The resulting yellow solution was diluted further with methanol before the cyclohexene substrate was added. Finally hydrogen peroxide (30% aqueous, diluted in methanol) was introduced slowly *via* syringe pump (final peroxide concentration: 70 mM). After reaction at room temperature overnight, oxidation products were analysed by gas chromatography, by comparison to authentic samples of the expected products.

Ligand variations

The results of turnover reactions with ligands **2**, **5**, **6** and **7** are summarized in Table 1, along with data obtained using two ligand precursors (alcohol **10** and dioxolanone-protected ligand **12b**) for comparison. The diol **15**, alcohol **16**, ketone **17** and epoxide **19** products of cyclohexene oxidation are formed at low levels. The products of ligand breakdown (alkyl anilines **9a–d** and benzaldehyde) are also observed; oxidative ligand breakdown is discussed below. While levels of dihydroxylation are low, control experiments confirm that the ligand is required for dihydroxylation to occur: control turnover reactions carried out in the absence of ligand give no diol product.

Ligand **2b** effects biomimetic dihydroxylation and allylic oxidation of cyclohexene **14** and other alkenes under these conditions as previously reported.[39] None of the *N*-methyl, *N*-*tert*-butyl and *N*-phenyl variants bring any increase in turnover yields: the bulkier *tert*-butyl derivative **2c** produces trace amounts of diol **15**, while the methyl (**2a**) and phenyl (**2d**) derivatives produce no detectable level of the desired diol product.

Reactions with the following ligand combinations were carried out to probe which parts of ligand **2** are most important to activity: amines **5** and **6**, disodium mandelate **7**·Na_2, the precursor alcohol **10**, and the dioxolanone-protected ligand **12b** (Table 1). With the tridentate ligand **5**, the main products are cyclohexenol **16**, cyclohexenone **17** and *N*-ethylaniline **9b**; trace amounts of diol **15** are seen and no epoxide **19**. The reaction using amine **6** in tandem with disodium mandelate **7**·Na_2 and iron(II) acetate gives benzaldehyde as the major product, from the oxidative breakdown of the ligand; smaller amounts of *N*-ethylaniline **9b** were observed relative to the reactions of the ligands **2a–d**, and only trace amounts of diol **15** and allylic oxidation products **16** and **17** were observed. Using amine **6** on its own does not generate any diol product, while disodium mandelate (**7**·Na_2) as sole ligand produces almost half the amount of diol produced by ligand **2b**. The protected ligand **12b** (in which both oxygen atoms are masked) gives primarily *N*-ethylaniline **9b** and allylic oxidation products, while the precursor alcohol **10** gives mostly allylic oxidation products, with trace amounts of diol **15**. These experiments suggest that the oxygen donors in the ligand **2b** are key to diol formation. Anilines are not particularly

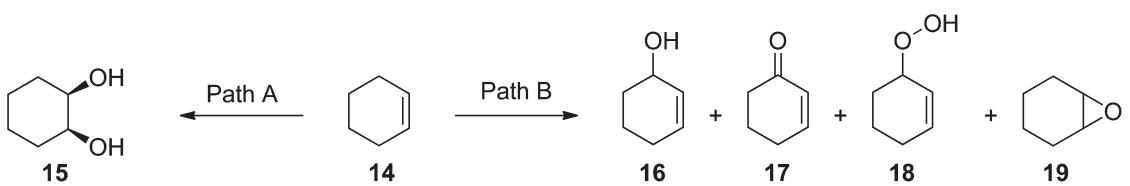

Scheme 3 Oxidation products from reaction of cyclohexene **14**: biomimetic dihydroxylation to give *cis*-cyclohexane-1,2-diol **15** (Path A) *vs.* Fenton-type reactivity to give allylic oxidation products alcohol **16**, ketone **17** and sometimes hydroperoxide **18** and epoxide **19** (Path B). The epoxide may be hydrolysed to the *trans*-diol, so the stereochemistry of diol product was confirmed unambiguously by spiking with authentic samples and separation of isomers on the polar BP-20 column (see Experimental for further details).

Table 1 Variation of product yield with ligands **2–12**[a,b]

Ligand	**15**[c]	**16**[c]	**17**[c]	**19**[c]	RNHPh[c]	PhCHO[c]
2a	—	0.10	0.10	—	1.26	—
2b	0.63	0.21	0.32	0.10	1.63	—
2c	<0.10	0.42	1.51	<0.10	4.11	—
2d	—	<0.10	<0.10	—	—	—
5	<0.10	0.43	0.76	—	1.46	—
6[d]	—	0.10	0.22	—	1.72	—
7·Na_2 [d]	0.13	0.21	0.22	0.13[e]	—	3.13
7·Na_2 + **6**[f]	<0.10	<0.10	0.10	—	0.34	7.06
10	0.13	0.63	1.98	<0.10[e]	—	—
12b	<0.10	0.21	0.10	—	0.52	—
—[g]	—	0.10	0.44	—	—	—

[a] Initial ratio catalyst : H_2O_2 : substrate 1 : 10 : 1000 (**2** (9.6 μmol) : iron(II) acetate (9.6 μmol) : hydrogen peroxide (96 μmol) : cyclohexene (9.6 mmol) : solvent methanol (30 mL)). See Experimental section for more details. [b] Catalyst prepared *in situ* from ligand and iron(II) acetate in methanol; reaction run in methanol. [c] Percentage yield relative to H_2O_2, the limiting reagent. Turnover number (μmol product produced per μmol catalyst) can be derived by dividing these percentage yields by 10. Percentage conversion of alkene = percentage yield/100. [d] Two equivalents relative to $Fe(OAc)_2$. [e] Hydrolysed to and identified as the *trans*-diol product. [f] **7**·Na_2 (1 eq) and **6** (1 eq) were dissolved in methanol and stirred while $Fe(OAc)_2$ (1 eq) was added. [g] Control contains no ligand. All values shown are the averages of at least three repetitions.

basic amines due to the electron withdrawing effect of partial delocalisation of the nitrogen lone pair into the phenyl ring, so the truncated ligands **5** and **6** are likely to bind weakly to iron. Considered together, these results suggest that the most likely reason for the low levels of dihydroxylation seen with ligands **2** is weak binding of the aniline moiety to iron.

Variation in reaction conditions

In addition to the ligand, a range of other reaction variables were investigated in the effort to improve diol yields.

Concentration: Varying the concentration of the complex and substrate also influences reaction outcome. Diluting the solution results in more diol formation and less allylic oxidation: diol formation increases from <0.10% to 0.63% when the concentrations of complex and substrate are lowered from 1.6 mM complex/95 mM substrate to 0.32 mM/32 mM. The substrate is used in 1000-fold excess relative to the complex, increasing the likelihood of an activated iron(II) complex reacting with a substrate molecule in dilute solution, and at the same time reducing the chances of an activated iron complex coming into contact with an unactivated iron(II) complex or free iron(II), which could lead to the breakdown of the peroxide species and generate radicals in a Fenton-type reaction.[51] The time period over which the dilute oxidant (hydrogen peroxide, 30% aqueous) was added was also varied to assess the effect on conversion. The addition time was varied from 30 minutes to 24 hours using a syringe pump. The yield of diol product increased with addition times up to 4 hours but no further increase was achieved by extending the addition time.

Temperature: Fenton and Fenton-type reactions are temperature-dependent and occur with greater efficiency at higher temperatures.[52] Thus turnover reactions were performed at low temperature, forming the iron-ligand complex and diluting as above, then cooling the solution to 0, −41 or −78 °C prior to addition of substrate and the oxidant (hydrogen peroxide, diluted and added over 4 hours as detailed above). The reaction was then stirred at the specified temperature for 12–14 hours before being allowed to warm to room temperature over 6 hours. Reaction at 0 °C gave product yields and ratios little changed from the room temperature reaction. However at −41 °C and −78 °C, only trace amounts of the allylic oxidation products were observed and the *cis*-diol **15** was the major substrate-derived product, formed in 0.71% yield at −41 °C (*versus* 0.63% at room temperature). The other major product was the ligand breakdown product *N*-ethylaniline **9b**, formed at a reduced level relative to the room temperature reaction (0.51% *vs.* 1.63%).

pH: The reaction is sensitive to pH, which is unsurprising given the nature of the ligand. The ligand is deprotonated at its carboxylic acid and adjacent alcohol prior to complexation with iron(II) by treatment with sodium hydride, and the sodium salt of the ligand stored in a dessicator overnight to remove any water. The oxidation reaction was found to tolerate a slight excess of sodium hydride (3–4 equivalents) however addition of 6 equivalents resulted in no reaction. The addition of only one equivalent gave reduced yields of diol product (<0.10 μmol) and no diol product at all was observed in the presence of protonated ligand or under acidic conditions.

Solvent: Acetonitrile is commonly used in iron-based oxidations given the potential for competing solvent oxidation when methanol is used. However the iron complexes derived from ligands **2a–d** are poorly soluble in acetonitrile and gave no diol product when tested under the alternative conditions of iron(II) acetate–acetonitrile.

In combination, these results demonstrate a very delicate balance of steric and electronic factors which affect the oxidative ability of this system.

Ligand degradation

The same Fenton-type pathways that result in allylic oxidation of the alkene substrate could also promote destruction of the peptidomimetic ligands, which would give rise to the observed by-products *N*-alkylanilines **9a–d** and benzaldehyde. Zs-Nagy and Floyd have reported the quenching effects of amino acids on hydroxyl radicals generated in the presence of iron(II) in Fenton-type chemistry.[53] This study, and subsequent work by Stadtman and Berlett,[54] demonstrated that amino acids can be oxidatively degraded by the combination of iron(II) and hydrogen peroxide *via* various pathways including oxidative decarboxylation, deamination and hydrogen abstraction. We believe similar processes contribute to the low activity of our system, as ligands **2** are amino acids (although the amino and carboxy termini are remote from each other).

Subjecting ligand **2b** to 'turnover' conditions without an alkene substrate (*i.e.* combining with iron(II) acetate and adding hydrogen peroxide at the same concentrations as for alkene oxidation reactions) gave a mixture of products. This was shown by LCMS (ESI†) to include compounds **20–23**, the products of oxidative decarboxylation (**20**), dehydration (**21**), deamination (**22**) and decarboxylation plus deamination (**23**) (Scheme 4). None of

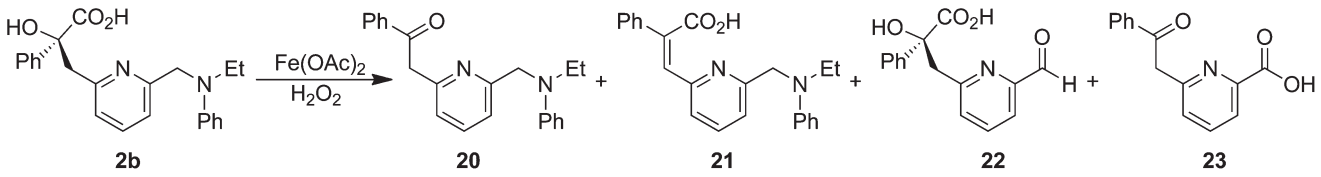

Scheme 4 Oxidative breakdown products of the ligand **2b**, the products of oxidative decarboxylation (**20**), dehydration (**21**), deamination (**22**) and decaboxylation–deamination (**23**), analogous to reaction pathways observed previously for the breakdown of simple amino acids under similar conditions.[53,54]

the starting ligand **2b** survived after 17 hours under these conditions. Control experiments subjecting ligand **2b** to dilute hydrogen peroxide without iron returned most of the ligand (>80%) unreacted plus low levels of amino-ketone **20** (ESI†).

Mechanistic conclusions

We propose that the oxidation reactions observed with ligands **2**, **5**, **6** and **7** follow a mechanism akin to those proposed by Que and others for the reaction of polyamine–iron complexes, hydrogen peroxide and alkene substrates.[31–35] Thus reaction begins with formation of an iron-peroxo intermediate (L_nFe^{III}–OOH, **24**). This intermediate can promote the allylic oxidation pathways itself or break down *via* several competing pathways (Scheme 5), giving rise to a number of possible oxidants: (1) L_nFe–OOH **24** itself; (2) the peroxy radical (˙OOH) formed *via* homolysis of the Fe–O bond in **24** (reaction a); (3) the hydroxy radical ˙OH, generated by bimolecular reaction of two peroxy radicals (reaction b); (4) an iron(IV)-oxo species L_nFe^{IV}=O **25**, generated by homolysis of the O–O bond in **24** (reaction c); (5) an iron(V)-oxo species L_nFe^{V}=O **26**, arising from heterolysis of the O–O bond in **24** (reaction d).[16]

The nature of L_n dictates which of these pathways predominate and controls the outcome of the reaction. With the ligands used in this study, pathways a and b appear to be dominant, leading to various oxidation products *via* radical mechanisms. Formation of the *cis*-diol product **15** indicates that an alternative 'biomimetic' reaction *via* **25** (or **26**) is also operating under these conditions, but only at very low levels.

Furthermore we postulate that the breakdown of ligand **2b** to the products **20–23** follows—at least in part—an intramolecular mechanism *via* **25** or **26**. The hydroxy and peroxy radical intermediates generated *via* reactions a and b offer one route to products **20–23**, *via* mechanisms analogous to those characterised by Stadtman and Berlett.[54] However under all the conditions investigated in the current study, release of *N*-ethylaniline **9b** *via* oxidative deamination of ligand **2b** occurs to a greater extent than allylic oxidation of cyclohexene, even though the alkene is present in 1000-fold excess. The amine product **9b** is observed even under conditions in which the allylic oxidation reaction is all but abolished (reduced temperature). One explanation for these observations is that at least one step of the oxidative degradation of ligand **2b** occurs while the ligand is bound to the iron centre: intramolecular iron-mediated oxidation would explain why even in high substrate concentration, oxidation of the ligand occurs preferentially. It would also explain why when the Fenton pathway has all but been eliminated, ligand oxidation occurs and *cis*-diol yield is not substantially increased.

A substantial portion of the oxidising potential introduced in these reactions (which employ a 10-fold excess of hydrogen peroxide relative to the iron complex) must also be lost elsewhere. Oxidation of the solvent methanol is the most likely explanation, although the likely oxidation products were not directly observed during this study. Future work will focus on the use of alternative iron salts (*e.g.* iron(II) triflate, iron(II) tetrafluoroborate) to improve complex solubility and allow turnover reactions to be performed in acetonitrile solutions.

Experimental

General experimental

Solvents were purified and distilled under nitrogen prior to use: dichloromethane (DCM) and methanol from calcium hydride; tetrahydrofuran (THF) from sodium metal and benzophenone ketyl radical. Alkene substrates were distilled from calcium hydride and stored over 4 Å molecular sieves. When required, solvents were degassed using the freeze–thaw method in three cycles. Thin layer chromatography (TLC) was carried out on aluminium-backed plates, pre-coated with Merck silica gel 60 F_{254}; plates were visualised using an ultraviolet lamp and/or by staining with ninhydrin solution (0.3% w/v in 97 : 3 *n*-BuOH–AcOH) or phosphomolybdic acid (0.01% phosphomolybdic acid, 0.001% ceric sulphate, H_2O–H_2SO_4–EtOH 20 : 1 : 40) and heating. Retention factors are quoted to the nearest 0.05. Flash chromatography was carried out using Ajax Finechem silica gel 230–400 mesh. Melting points were recorded on a GallenKamp melting point apparatus. Optical rotations were measured on a Perkin Elmer model 341 Polarimeter with a sodium lamp at 589 nm in a 1.0 or 0.5 dm cell at the concentration (g per 100 mL) and temperature indicated. Infrared spectra were measured on a Shimadzu Bio-Rad 8400S on a sodium chloride

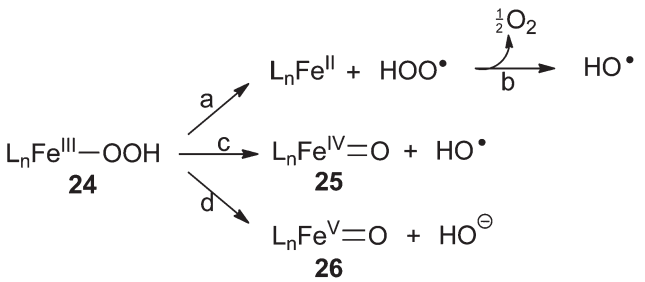

Scheme 5 Potential breakdown pathways for the L_nFe^{III}–OOH intermediate **24**, generating five potential oxidants in non-heme iron systems.[16]

plate (oils), KBr disc, or in solution in the solvent indicated; absorbances are quoted in wavenumbers (cm^{-1}) and recorded as strong (s), medium (m), weak (w) and broad (br). NMR spectra were recorded on Bruker DPX 200, DPX 300 and DPX 400 spectrometers; chemical shifts are reported in parts per million (ppm) from tetramethylsilane (TMS) and referenced to TMS or the appropriate residual solvent peak. ^{1}H NMR data are quoted as the signal (ppm), relative integral, multiplicity (singlet s, doublet d, triplet t, quartet q, double doublet dd, multiplet m) and coupling constant J (quoted in hertz to the nearest 0.5 Hz). ^{13}C NMR data (50, 75 or 100 MHz) are quoted as the signal (ppm) to the nearest 0.1 ppm. Low resolution mass spectra were recorded on a Finnigan LCQ MS Detector (ESI); major peaks are recorded as mass to charge (m/z) followed by the height of the peak as a percentage of the base peak and assignment. High resolution mass spectra were recorded on a Bruker Apex II FTICR mass spectrometer. LCMS was carried out using a Thermo Separation Products SCM 1000 vacuum membrane degasser, Thermo Separation Products Spectra System, P4000 pump and AS3000 autosampler, a Phenomenex Luna C18(2) column (2.0 × 150 mm ID, 5 μm), and a ThermoQuest Finnigan LCQ DecaMass spectrometer. GC analyses were performed on a Hewlett-Packard 5890 Series II gas chromatograph using an HP-1ms column (30 m × 0.25 mm ID, 0.25 μm; ramping 70 to 160 °C at 12 °C min^{-1}) and a Hewlett-Packard 5890A gas chromatograph with a BP-20 column (25 m × 0.22 mm ID, 0.25 μm; ramping 40 to 220 °C at 12 °C min^{-1}), each equipped with split/splitless capillary inlet and flame ionisation detector (FID) and controlled using ChemStation software. GCMS was carried out using a Finnigan PolarisQ fitted with a ZB–5 column (15 m × 0.25 mm ID, 0.10 μm; ramping 40 to 120 °C at 10 °C min^{-1} or 40 to 260 °C at 20 °C min^{-1}) connected to a Thermo-Finnigan Polaris Q ion trap mass spectrometer.

Synthesis of ligands

(2*S*,5*S*)-2-*tert*-Butyl-5-((6-((methyl(phenyl)amino)methyl)-pyridin-2-yl)methyl)-5-phenyl-1,3-dioxolan-4-one 12a. A solution of *N*-methylaniline **9a** (0.16 mL, 1.49 mmol) in THF (10 mL) was cooled to 0 °C and a solution of *n*-BuLi in hexane (1.5 M, 1.19 mL, 1.78 mmol) was added *via* syringe. The solution was stirred at 0 °C for 20 minutes before DMPU (0.22 mL, 1.78 mmol) was added and the solution was stirred for a further 20 minutes. The now yellow solution was cooled to −78 °C and added *via* cannula to a solution of the bromide **11** (0.50 g, 1.24 mmol) in THF (10 mL) also at −78 °C. The resulting yellow solution was stirred at −78 °C for 5 hours, monitored by TLC (cyclohexane–ethyl acetate 5 : 1). The solution was allowed to warm to room temperature slowly overnight then poured onto half-saturated aqueous ammonium chloride solution. The aqueous phase was extracted with diethyl ether (3 × 5 mL). The organic phases were combined, washed with brine (4 mL), and dried ($MgSO_4$). The solvent was removed *in vacuo* to give a crude yellow oil, which was purified by column chromatography (cyclohexane–ethyl acetate 20 : 1) to afford the title compound as a pale yellow semi-solid (0.38 g, 84%). R_f 0.46 (cyclohexane–ethyl acetate 5 : 1); $[\alpha]_D^{20}$ −53.8 ($CHCl_3$, c 0.93); ν_{max} (NaCl, cm^{-1}): 2978 (s), 2952 (s), 1787 (s), 1448 (m), 1383 (m), 1221 (s); δ_H (300 MHz, $CDCl_3$): 0.88 (9H, s, $C(CH_3)_3$), 3.11 (3H, s, NCH_3), 3.37 (1H, d, J = 14.5 Hz, 1 of $CH_2CC_6H_5$), 3.69 (1H, d, J = 14.5 Hz, 1 of $CH_2CC_6H_5$), 4.61 (2H, s, $CH_2NC_6H_5$), 4.79 (1H, s, $CHC(CH_3)_3$), 6.60–6.98 (3H, m, 3 of NC_6H_5), 6.98 (1H, d, J = 7.5 Hz, CH_{Pyr}), 7.06 (1H, d, J = 7.5 Hz, CH_{Pyr}), 7.21 (2H, t, J = 7.5 Hz, 2 of NC_6H_5), 7.35 (3H, m, 3 of CC_6H_5), 7.52 (1H, t, J = 7.5 Hz, CH_{Pyr}), 7.77 (2H, m, 2 of CC_6H_5); δ_C (75 MHz, $CDCl_3$): 23.6, 34.9, 39.2, 48.4, 58.6, 82.2, 109.6, 112.1, 116.7, 119.2, 122.5, 125.0, 128.0, 128.3, 129.2, 137.1, 139.1, 149.1, 155.1, 159.2, 173.4; m/z (ES+): 883 (25%, $[2M + Na]^+$), 453 (100%, $[M + Na]^+$), 431 (65%, $[MH]^+$); HRMS (ES+): $C_{27}H_{31}N_2O_3^+$ ($[MH^+]$) requires 431.2335, found 431.2345.

(2*S*,5*S*)-2-*tert*-Butyl-5-((6-((*tert*-butyl(phenyl)amino)methyl)-pyridin-2-yl)methyl)-5-phenyl-1,3-dioxolan-4-one 12c. *tert*-Butylaniline **9c** (43 mg, 0.28 mmol) in THF (4.0 mL) was cooled to −41 °C and a solution of *n*-BuLi in hexane (1.42 M, 0.24 mL, 0.35 mmol) was added *via* syringe. The solution was stirred at −5 °C for 45 minutes then added *via* cannula to a solution of the bromide **11** (100 mg, 0.24 mmol) in THF (4.0 mL) also at −5 °C. The resulting yellow solution was stirred at −5 °C for 4 hours, monitored by TLC (cyclohexane–ethyl acetate 5 : 1). The solution was allowed to warm to room temperature then poured onto half-saturated aqueous ammonium chloride solution. The aqueous phase was then extracted with DCM (3 × 4 mL). The organic phases were combined and washed with brine (3 mL), and dried ($MgSO_4$). The solvent was removed *in vacuo* to give an orange oil which was purified by column chromatography (cyclohexane–ethyl acetate 12 : 1) to afford the title compound as a pale yellow oil (45 mg, 40%). R_f 0.5 (cyclohexane–ethyl acetate, 5 : 1); $[\alpha]_D^{20}$ −43.1 ($CHCl_3$, c 0.65); ν_{max} (NaCl): 3065 (w), 2963 (s), 2961 (s), 1785 (s), 1590 (m), 1574 (m), 1214 (s); δ_H (300 MHz, $CDCl_3$): 0.81 (9H, s, $CHC(CH_3)_3$), 1.18 (9H, s, $NC(CH_3)_3$), 3.25 (1H, d, J = 14.5 Hz, 1 of $CH_2CC_6H_5$), 3.42 (1H, d, J = 14.5 Hz, 1 of $CH_2CC_6H_5$), 4.50 (3H, s, $CH_2NC_6H_5$, $CHC(CH_3)_3$), 6.87 (1H, d, J = 7.5 Hz, CH_{Pyr}), 7.10–7.39 (8H, m, 3 of CC_6H_5 and 5 of NC_6H_5), 7.47 (1H, t, J = 7.5 Hz, CH_{Pyr}), 7.51 (1H, d, J = 7.5 Hz, CH_{Pyr}), 7.73 (2H, m, 2 of CC_6H_5); δ_C (75 MHz, $CDCl_3$): 23.6, 28.4, 34.9, 48.7, 56.1, 57.1, 82.3, 109.5, 120.8, 121.8, 124.5, 124.9, 127.9, 128.2, 128.2, 129.3, 136.6, 139.4, 149.8, 153.8, 162.2, 173.3; m/z (ES+): 967 (5%, $[2M + Na]^+$), 473 (100%, $[MH]^+$); HRMS (ES+): $C_{30}H_{37}N_2O_3^+$ ($[MH]^+$) requires 473.2804, found: 473.2819.

(2*S*,5*S*)-2-*tert*-Butyl-5-((6-((diphenylamino)methyl)pyridin-2-yl)methyl)-5-phenyl-1,3-dioxolan-4-one 12d. A solution of diphenylamine **9d** (0.35 g, 2.08 mmol) in THF (12.0 mL) was cooled to 0 °C and a solution of *n*-BuLi in hexane (1.5 M, 1.7 mL, 2.5 mmol) was added *via* syringe. The solution was stirred at 0 °C for 20 minutes, before DMPU (0.3 mL, 2.5 mmol) was added and the solution was stirred for a further 20 minutes. The resulting yellow solution was cooled to −15 °C then added *via* cannula to a solution of the bromide **11** (0.70 g, 1.73 mmol) in THF (12.0 mL) also at −15 °C. The resulting yellow solution was stirred at −15 °C for 5 hours, monitored by TLC (cyclohexane–ethyl acetate 5 : 1). The solution was allowed to warm to room temperature overnight, then poured onto half-

saturated aqueous ammonium chloride solution. The aqueous phase was extracted with DCM (3 × 4 mL) and the organic phases were combined, washed with brine (5 mL), and dried ($MgSO_4$), then concentrated *in vacuo* to give an orange oil. The crude product was purified by column chromatography (cyclohexane–ethyl acetate 10 : 1) to afford the title compound as a white solid (0.70 g, 82%). R_f 0.5 (cyclohexane–ethyl acetate 5 : 1); m.p. 105–108 °C; $[\alpha]_D^{20}$ −65.7 ($CHCl_3$, *c* 0.82); ν_{max} (NaCl): 3060 (w), 2962 (s), 2961 (s), 1793 (s), 1590 (m), 1577 (m), 1178 (s); δ_H (300 MHz, $CDCl_3$): 0.86 (9H, s, $C(CH_3)_3$), 3.36 (1H, d, J = 14.5 Hz, 1 of $CH_2CC_6H_5$), 3.67 (1H, d, J = 14.5 Hz, 1 of $CH_2CC_6H_5$), 4.77 (1H, s, $CHC(CH_3)_3$), 5.06 (2H, s, $CH_2NC_6H_5$), 6.60–6.94 (3H, m, 2 of NC_6H_5, 1 of CC_6H_5), 7.04 (4H, m, 4 of NC_6H_5), 7.20–7.41 (8H, m, 2 of CC_6H_5, 4 of NC_6H_5, 2 × CH_{Pyr}), 7.49 (1H, t, J = 7.5 Hz, CH_{Pyr}), 7.76 (2H, d, J = 1.5 Hz, 2 of CC_6H_5); δ_C (75 MHz, $CDCl_3$): 23.6, 35.0, 48.3, 58.3, 82.2, 109.8, 119.5, 120.6, 121.7, 122.6, 125.0, 128.0, 128.3, 129.4, 137.2, 139.1, 147.8, 155.1, 159.5, 173.5; *m*/*z* (ES+): 515 (35%, $[M + Na]^+$), 493 (100%, $[MH]^+$); HRMS (ES+): $C_{32}H_{33}N_2O_3^+$ ($[MH]^+$) requires 493.2491, found 493.2491.

(*S*)-2-Hydroxy-3-(6-((methyl(phenyl)amino)methyl)pyridin-2-yl)-2-phenylpropanoic acid 2a. Aqueous lithium hydroxide solution (1 M, 0.15 mL, 0.15 mmol) was added to a solution of **12a** (50 mg, 0.12 mmol) in THF (0.1 mL) producing two phases. The reaction mixture was heated at reflux (105 °C) for 17 hours during which time it became homogeneous. The resulting solution was allowed to cool to room temperature and adjusted to pH 7 using aqueous hydrochloric acid (1 M). The solvent was removed *in vacuo* to give a pale yellow solid which was triturated with DCM (3 × 3 mL). The DCM phase was reduced *in vacuo* to afford the crude product as a pale yellow foam, which was triturated with ether (3 × 0.5 mL). The solvent was decanted to give the title compound as an off-white solid (43 mg, 81%); R_f 0.5 (DCM–MeOH 10 : 1); m.p. 76–82 °C; $[\alpha]_D^{20}$ −33.2 ($CHCl_3$, *c* 0.50); ν_{max} ($CHCl_3$): 3355 (w), 1604 (s), 1573 (m), 1504 (m), 1456 (w), 1447 (w), 1371 (m); δ_H (300 MHz, CD_3OD): 3.06 (3H, s, NCH_3), 3.52 (1H, d, J = 14.0 Hz, 1 of $CH_2CC_6H_5$), 3.72 (1H, d, J = 14.5 Hz, 1 of $CH_2CC_6H_5$), 4.56 (2H, s, CH_2N), 6.60–6.67 (3H, m, 3 of NC_6H_5), 6.94 (1H, d, J = 7.5 Hz, CH_{Pyr}), 7.10–7.27 (6H, m, 3 of CC_6H_5, CH_{Pyr}, 2 of NC_6H_5), 7.49 (1H, t, J = 7.5 Hz, CH_{Pyr}), 7.69–7.72 (2H, m, 2 of CC_6H_5); δ_C (75 MHz, $CDCl_3$): 39.5, 44.8, 58.65, 81.0, 112.6, 117.0, 118.8, 123.7, 126.5, 127.8, 128.4, 129.6, 137.8, 143.6, 149.3, 158.0, 159.3, 179.9; *m*/*z* (ES+): 385 (100%, $[M + Na]^+$), 363 (100%, $[MH]^+$); HRMS (ES+): $C_{22}H_{23}N_2O_3^+$ ($[MH]^+$) requires 363.1709, found 363.1710.

(*S*)-3-(6-((*tert*-Butyl(phenyl)amino)methyl)pyridin-2-yl)-2-hydroxy-2-phenylpropanoic acid 2c. Following the procedure outlined above for preparation of **2a** from **12a**, **12c** (0.26 g, 0.6 mmol) gave **2c** as an off-white solid (0.20 g, 90%). R_f 0.2 (DCM–MeOH 10 : 1); m.p. 98–100 °C; $[\alpha]_D^{20}$ −56.5 ($CHCl_3$, *c* 0.69); ν_{max} ($CHCl_3$): 3200 (w), 1629 (s), 1596 (s), 1575 (m), 1491 (m), 1460 (m), 1365 (s); δ_H (300 MHz, $CDCl_3$): 1.08 (9H, s, $NC(CH_3)_3$), 3.35 (1H, d, J = 14.0 Hz, 1 of $CH_2CC_6H_5$), 3.43 (1H, d, J = 14.5 Hz, 1 of $CH_2CC_6H_5$), 4.33 (2H, s, $CH_2NC_6H_5$), 6.87–6.95 (2H, m, 2 of NC_6H_5), 7.06–7.33 (7H, m, 3 of CC_6H_5, 3 of NC_6H_5, CH_{Pyr}), 7.53–7.64 (2H, m, 2 × CH_{Pyr}), 7.55 (2H, m, 2 of CC_6H_5); δ_C (75 MHz, $CDCl_3$): 26.2, 42.1, 56.5, 56.6, 78.5, 115.4, 118.0, 120.3, 122.2, 124.0, 125.1, 125.9, 127.1, 134.5, 141.0, 147.0, 155.6, 158.1, 177.2; *m*/*z* (ES+): 427 (50%, $[M + Na]^+$), 411 (45%, $[M + Li]^+$), 405 (100%, $[MH]^+$); HRMS (ES+): $C_{25}H_{28}N_2O_3Li^+$ requires 411.2260, found 411.2266.

(*S*)-3-(6-((Diphenylamino)methyl)pyridin-2-yl)-2-hydroxy-2-phenyl propanoic acid 2d. Following the procedure outlined above for preparation of **2a** from **12a**, but using methanol (0.2 mL) as the co-solvent in place of THF, **12d** (0.22 g, 0.5 mmol) was converted to **2d** as a white solid (0.18 g, 90%). R_f 0.2 (DCM–MeOH 10 : 1); m.p. 112–117 °C; $[\alpha]_D^{20}$ −14.0 ($CHCl_3$, *c* 0.60); δ_H (300 MHz, CD_3OD): 3.64 (1H, d, J = 14.5 Hz, 1 of $CH_2CC_6H_5$), 3.53 (1H, d, J = 14.5 Hz, 1 of $CH_2CC_6H_5$), 4.57 (2H, s, $CH_2NC_6H_5$), 6.65 (2H, m, 2 of NC_6H_5), 7.05 (4H, d, 1 Hz, 4 of NC_6H_5), 7.12–7.29 (9H, m, 3 of CC_6H_5, 4 of NC_6H_5, 2 × CH_{Pyr}), 7.54 (1H, t, J = 7.0 Hz, CH_{Pyr}), 7.76 (2H, d, J = 1.0 Hz, CC_6H_5); δ_C (75 MHz, CD_3OD–$CDCl_3$): 45.6, 59.4, 82.1, 121.2, 122.1, 123.2, 125.2, 127.7, 128.7, 129.6, 130.9, 140.1, 144.0, 149.2, 159.5, 159.6, 179.3; *m*/*z* (ES+): 447 (60%, $[M + Na]^+$), 425 (100%, $[MH]^+$); HRMS (ES+): $C_{27}H_{25}N_2O_3^+$ ($[MH]^+$) requires 425.1865, found 425.1874.

***N*,*N*′-(Pyridine-2,6-diylbis(methylene))bis(*N*-ethylaniline) 5.** *N*-Ethylaniline **9b** (0.12 mL, 0.90 mmol) was dissolved in THF (2.0 mL) and the solution was cooled to 0 °C. *n*-BuLi (1.5 M, 0.66 mL, 1.0 mmol) was added and the solution was stirred for 20 minutes at 0 °C. DMPU (0.12 mL, 1.0 mmol) was added and the solution was stirred for a further 20 minutes, then added *via* cannula to a solution of 2,6-dibromomethylpyridine (100 mg, 0.4 mmol)[41] in THF (4.0 mL) cooled to −41 °C. The solution was stirred at −41 °C for 16 hours after which time it was poured onto half-saturated aqueous ammonium chloride solution (3 mL). The aqueous phase was washed with ethyl acetate (3 × 10 mL) and the organic layers combined and washed with brine, dried ($MgSO_4$) and reduced *in vacuo* to yield an orange oil. The crude product solidified on standing and was recrystallised from ethyl acetate to afford the title compound as a white solid (100 mg, 73%); R_f 0.3 (hexane–ethyl acetate, 5 : 1); m.p.: 151–156 °C; ν_{max} ($CHCl_3$): 3002 (w), 2970 (m), 1600 (s), 1573 (s), 1500 (s), 1348 (s), 1245 (m); δ_H (200 MHz, $CDCl_3$): 1.17 (6H, t, J = 7.0 Hz, 2 × (NCH_2CH_3)), 3.46 (4H, q, J = 7.0 Hz, 2 × (NCH_2CH_3)), 4.60 (4H, s, 2 × ($CH_2NC_6H_5$)), 6.60–6.65 (6H, m, 6 of 2 × (NC_6H_5)), 7.01–7.17 (6H, m, 2 of 2 × (NC_6H_5), 2 × CH_{Pyr}), 7.44 (1H, t, J = 7.5 Hz, CH_{Pyr}); δ_C (50 MHz, $CDCl_3$): 12.8, 46.1, 56.8, 112.6, 116.8, 119.3, 129.8, 137.9, 148.6, 160.0; *m*/*z* (ES^+): 346 (100%, $[MH]^+$), 225 (27%, $[M - PhNEt]^+$); HRMS (ES^+): $C_{23}H_{28}N_3^+$ ($[MH]^+$)requires: 346.2283, found 346.2279.

***N*-Ethyl-*N*-(pyridin-2-ylmethyl)aniline 6.** *N*-Ethylaniline **9b** (0.81 mL, 1.46 mmol) was dissolved in THF (4.0 mL) and stirred at 0 °C while *n*-BuLi (1.5 M, 1.95 mL, 2.92 mmol) was added *via* syringe. The resulting yellow solution was stirred at 0 °C for 20 minutes, then DMPU (0.35 mL, 1.46 mmol) was added and stirring continued for a further 10 minutes. The solution was cooled to −78 °C and added dropwise *via* cannula to a

suspension of 2-(chloromethyl)pyridine (200 mg, 1.22 mmol)[49] in THF (4.0 mL). The reaction mixture was allowed to slowly warm to room temperature while stirring overnight. The clear, orange solution that resulted was poured onto half-saturated aqueous ammonium chloride solution (5 mL). The aqueous phase was extracted with ethyl acetate (3 × 5 mL) and the combined organic extracts were washed with brine (5 mL), dried ($MgSO_4$) and reduced *in vacuo* to give the crude product as an orange oil. The product was purified by column chromatography (hexane–ethyl acetate 5 : 1) to give the pure product as a bright yellow oil (100 mg, 40%); R_f 0.15 (hexane–ethyl acetate 5 : 1); ν_{max} ($CHCl_3$): 3089 (w), 2950 (s), 1600 (s), 1585 (s) 1492 (s), 1350 (s), 1272 (m); δ_H (200 MHz, $CDCl_3$): 1.14 (3H, t, J = 7.0 Hz, CH_2CH_3), 3.44 (2H, q, J = 7.0 Hz, CH_2CH_3), 4.53 (2H, s, $NCCH_2$), 6.55–6.61 (3H, m, 3 of NC_6H_5), 7.01–7.13 (4H, m, 2 of NC_6H_5, 2 × CH_{Pyr}), 7.47 (1H, dt, J = 7.5 Hz, 8.0 Hz, CH_{Pyr}), 8.49 (1H, q, J = 4.0 Hz, CH_{Pyr}); δ_C (50 MHz, $CDCl_3$): 12.6, 46.1, 56.7, 112.6, 116.8, 120.4, 121.2, 129.6, 137.2, 148.5, 149.9, 160.2; *m/z* (ES^+): 213 (100%, $[MH]^+$); HRMS (ES^+): $[C_{14}H_{17}N_2]^+$ requires 213.1392, found 213.1382.

We have reported the synthesis and characterisation of compounds **2b** and **12b** previously.[39] Synthetic procedures and data for these compounds are included in the ESI† for reference.

Oxidative turnover reactions

Ligand (0.13 mmol) was dissolved in anhydrous DCM (0.75 mL) and treated with NaH (12 mg, 0.53 mmol). After stirring for 45 minutes at room temperature the solvent was removed *in vacuo* to give a white powder. A solution of iron(II) acetate (1.7 mg, 9.5 μmol) in degassed, dry methanol (0.1 mL) was added to a solution of the disodium salt of the ligand (4.0 mg, 9.5 μmol) in methanol (0.2 mL) under argon to give a yellow solution. The reaction was stirred for 20 minutes after which time it was diluted with methanol (30 mL) and the alkene substrate (9.5 mmol) was added. Hydrogen peroxide (30% aqueous, 97 μmol) in methanol (1.0 mL) was added by syringe pump over 4 hours. The reaction was stirred at room temperature for 24 hours. The solution was concentrated *in vacuo* and diluted with ethyl acetate (~2 mL) and passed through a short plug of silica to remove insolubles. An internal standard (*n*-decane) was added and products were analysed by GC or GCMS. Products were identified unambiguously in GC and GCMS analyses by comparison and spiking with authentic samples. Analysis on the HP-1s column achieved separation of products **15–19**, anilines **9a–d** and benzaldehyde; further analysis using the BP-20 column was required to confirm the stereochemistry of the cyclohexane-1,2-diol product **15** (R_t = 10.84 minutes for the *cis*-isomer **15** and 11.33 minutes for *trans*-cyclohexane-1,2-diol).

Ligand degradation experiments

a. Iron, ligand and oxidant: The sodium salt **2b-Na** (2.0 mg, 5.0 μmol) was dissolved in methanol (0.1 mL). Iron(II) acetate (0.85 mg, 5.0 μmol) in methanol (0.2 mL) was added, giving a yellow solution which was stirred at room temperature for 45 minutes. The solution was diluted with methanol (7.2 mL) and stirred at room temperature while hydrogen peroxide (30% aqueous, 50 μmol) in methanol (0.5 mL) was added over 4 hours. The reaction was stirred at room temperature for a

Table 2 Crystal data and structure refinement

Compound no.	**11**	**12d**
Empirical formula	$C_{20}H_{22}NO_3Br$	$C_{32}H_{32}N_2O_3$
Formula weight	404.30	492.60
Temperature	100(2) K	113(2) K
Wavelength	0.71073 Å	0.71073 Å
Crystal system	Monoclinic	Orthorhombic
Space group	$P2_1$ (#4)	$P2_12_12_1$ (#19)
Unit cell dimensions	a = 9.8965(17) Å α = 90° b = 8.9206(15) Å β = 113.274(2)° c = 11.355(2) Å γ = 90°	a = 10.0288(13) Å α = 90° b = 15.960(2) Å β = 90° c = 16.609(2) Å γ = 90°
Volume	920.9(3) $Å^3$	2658.5(6) $Å^3$
Z	2	4
Density (calculated)	1.458 Mg m^{-3}	1.231 Mg m^{-3}
Absorption coefficient	2.250 mm^{-1}	0.079 mm^{-1}
F(000)	416	1048
Crystal size	1.00 × 0.80 × 0.50 mm^3	0.50 × 0.50 × 0.50 mm^3
θ range for data collection	1.95–28.31°	1.77–26.00°
Index ranges	$-12 <= h <= 12$, $-11 <= k <= 11$, $-14 <= l <= 14$	$-12 <= h <= 12$, $-19 <= k <= 19$, $-20 <= l <= 20$
Reflections collected	7231	41 199
Independent reflections	3936 [R(int) = 0.0359]	2952 [R(int) = 0.0235]
Completeness to θ_{max}	92.9%	100.0%
Absorption correction	Semi-empirical from equivalents	Semi-empirical from equivalents
Max. and min. transmission	0.3991 and 0.1088	0.9616 and 0.8218
Refinement method	Full-matrix least-squares on F^2	Full-matrix least-squares on F^2
Data/restraints/parameters	3936/1/229	2952/0/337
Goodness-of-fit on F^2	1.004	1.039
Final R indices [$I > 2\sigma(I)$]	R_1 = 0.0438, wR_2 = 0.1007	R_1 = 0.0291, wR_2 = 0.0733
R indices (all data)	R_1 = 0.0490, wR_2 = 0.1020	R_1 = 0.0297, wR_2 = 0.0740
Flack×parameter	0.047(10)	— (Friedel pairs merged)
Largest diff. peak and hole	1.102 and −0.802 e $Å^{-3}$	0.236 and −0.138 e $Å^{-3}$

further 16 hours then concentrated *in vacuo*. Products were analysed by LCMS (water–acetonitrile with 0.2% TFA; gradient elution from 90–100% acetonitrile).

b. Iron-free control (ligand and oxidant): The sodium salt **2b-Na** (2.0 mg, 5.0 μmol) was dissolved in methanol (7.5 mL) and treated to hydrogen peroxide (30% aqueous, 50 μmol) in methanol (0.5 mL) as above. The reaction mixture was concentrated *in vacuo* and analysed by LCMS.

Crystallography

Crystal data were collected using a Bruker SMART APEX CCD area detector diffractometer. A full sphere of reciprocal space was scanned by phi-omega scans. Pseudo-empirical absorption correction based on redundant reflections was performed by the program SADABS.[55] The structures were solved by direct methods using SHELXS-97 (X-2) and refined by full matrix least-squares on F^2 for all data using SHELXL-97.[56] Friedel pairs were merged in **12d**. Hydrogen atoms were added at calculated positions and refined using a riding model. Their isotropic thermal displacement parameters were fixed to 1.2 times (1.5 times for methyl groups) the equivalent one of the parent atom. Anisotropic thermal displacement parameters were used for all non-hydrogen atoms. Further refinement details are listed in Table 2.

Acknowledgements

This work was supported by the Irish Research Council for Science, Engineering and Technology (IRCSET) *via* an Embark Award postgraduate scholarship to SMB, the Centre for Synthesis and Chemical Biology at University College Dublin under the Programme for Research in Third Level Institutions (PRTLI) administered by the HEA, and the University of Sydney.

References

1 D. H. R. Barton, *Chem. Soc. Rev.*, 1996, **25**, 237.
2 P. Gamez, P. G. Aubel, W. L. Driessen and J. Reedijk, *Chem. Soc. Rev.*, 2001, **30**, 376.
3 J. Piera and J. E. Backvall, *Angew. Chem., Int. Ed.*, 2008, **47**, 3506.
4 S. I. Murahashi and D. Zhang, *Chem. Soc. Rev.*, 2008, **37**, 1490.
5 T. D. H. Bugg, *Tetrahedron*, 2003, **59**, 7075.
6 M. Costas, M. P. Mehn, M. P. Jensen and L. Que, *Chem. Rev.*, 2004, **104**, 939.
7 W. Nam, *Acc. Chem. Res.*, 2007, **40**, 522.
8 P. C. A. Bruijnincx, G. van Koten and R. J. M. Klein Gebbink, *Chem. Soc. Rev.*, 2008, **37**, 2716.
9 A. Daruzzaman, I. J. Clifton, R. M. Adlington, J. E. Baldwin and P. J. Rutledge, *ChemBioChem*, 2006, **7**, 351.
10 M. L. Neidig and E. I. Solomon, *Chem. Commun.*, 2005, 5843.
11 M. M. Abu-Omar, A. Loaiza and N. Hontzeas, *Chem. Rev.*, 2005, **105**, 2227.
12 W. Ge, I. J. Clifton, J. E. Stok, R. M. Adlington, J. E. Baldwin and P. J. Rutledge, *J. Am. Chem. Soc.*, 2008, **130**, 10096.
13 W. Ge, I. J. Clifton, A. R. Howard-Jones, J. E. Stok, R. M. Adlington, J. E. Baldwin and P. J. Rutledge, *ChemBioChem*, 2009, **10**, 2025.
14 A. R. Grummitt, P. J. Rutledge, I. J. Clifton and J. E. Baldwin, *Biochem. J.*, 2004, **382**, 659.
15 E. L. Hegg and L. Que Jr., *Eur. J. Biochem.*, 1997, **250**, 625.
16 M. Costas, K. Chen and L. Que, *Coord. Chem. Rev.*, 2000, **200–202**, 517.
17 C. He and Y. Mishina, *Curr. Opin. Chem. Biol.*, 2004, **8**, 201.
18 J. M. Bollinger Jr and C. Krebs, *J. Inorg. Biochem.*, 2006, **100**, 586.
19 J. England, Y. Guo, E. R. Farquhar, V. G. Young Jr, E. Münck and L. Que Jr, *J. Am. Chem. Soc.*, 2010, **132**, 8635.
20 S. Ye and F. Neese, *Proc. Natl. Acad. Sci. U. S. A.*, 2011, **108**, 1228.
21 J. C. Price, E. W. Barr, B. Tirupati, J. M. Bollinger and C. Krebs, *Biochemistry*, 2003, **42**, 7497.
22 L. M. Hoffart, E. W. Barr, R. B. Guyer, J. M. Bollinger and C. Krebs, *Proc. Natl. Acad. Sci. U. S. A.*, 2006, **103**, 14738.
23 B. E. Eser, E. W. Barr, P. A. Frantom, L. Saleh, J. M. Bollinger, C. Krebs and P. F. Fitzpatrick, *J. Am. Chem. Soc.*, 2007, **129**, 11334.
24 K. Chen and L. Que Jr., *Angew. Chem., Int. Ed.*, 1999, **38**, 2227.
25 J. Bautz, P. Comba, C. L. de Laorden, M. Menzel and G. Rajaraman, *Angew. Chem., Int. Ed.*, 2007, **46**, 8067.
26 M. S. Chen and M. C. White, *Science*, 2007, **318**, 783.
27 K. Suzuki, P. D. Oldenburg and L. Que, *Angew. Chem., Int. Ed.*, 2008, **47**, 1887.
28 M. S. Chen and M. C. White, *Science*, 2010, **327**, 566.
29 J. England, M. Martinho, E. R. Farquhar, J. R. Frisch, E. L. Bominaar, E. Münck and L. Que, *Angew. Chem., Int. Ed.*, 2009, **48**, 3622.
30 J. England, Y. Guo, K. M. Van Heuvelen, M. A. Cranswick, G. T. Rohde, E. L. Bominaar, E. Münck and L. Que, *J. Am. Chem. Soc.*, 2011, **133**, 11880.
31 J. U. Rohde, J. H. In, M. H. Lim, W. W. Brennessel, M. R. Bukowski, A. Stubna, E. Munck, W. Nam and L. Que, *Science*, 2003, **299**, 1037.
32 B. B. Bassan, M. R. A. Blomberg, P. E. M. Siegbahn and L. Que Jr., *Angew. Chem., Int. Ed.*, 2005, **44**, 2939.
33 Y.-M. Lee, S. Hong, Y. Morimoto, W. Shin, S. Fukuzumi and W. Nam, *J. Am. Chem. Soc.*, 2010, **132**, 10668.
34 S. Hong, Y.-M. Lee, W. Shin, S. Fukuzumi and W. Nam, *J. Am. Chem. Soc.*, 2009, **131**, 13910.
35 A. Thibon, J. England, M. Martinho, V. G. Young, J. R. Frisch, R. Guillot, J.-J. Girerd, E. Münck, L. Que and F. Banse, *Angew. Chem., Int. Ed.*, 2008, **47**, 7064.
36 L. Que, *Acc. Chem. Res.*, 2007, **40**, 493.
37 I. Prat, J. S. Mathieson, M. Güell, X. Ribas, J. M. Luis, L. Cronin and M. Costas, *Nat. Chem.*, 2011, **3**, 788.
38 J. A. Krall, P. J. Rutledge and J. E. Baldwin, *Tetrahedron*, 2005, **61**, 137.
39 S. M. Barry and P. J. Rutledge, *Synlett*, 2008, 2172.
40 V. J. Dungan, Y. Ortin, H. Mueller-Bunz and P. J. Rutledge, *Org. Biomol. Chem.*, 2010, **8**, 1666.
41 V. J. Dungan, S. M. Wong, S. M. Barry and P. J. Rutledge, *Tetrahedron*, 2012, **68**, 3231.
42 A. Karlsson, J. V. Parales, R. E. Parales, D. T. Gibson, H. Eklund and S. Ramaswamy, *Science*, 2003, **299**, 1039.
43 D. Seebach and R. Naef, *Helv. Chim. Acta*, 1981, **64**, 2704.
44 C. F. Macrae, I. J. Bruno, J. A. Chisholm, P. R. Edgington, P. McCabe, E. Pidcock, L. Rodriguez-Monge, R. Taylor, J. van de Streek and P. A. Wood, *J. Appl. Crystallogr.*, 2008, **41**, 466.
45 A. R. Johnson, C. C. Cummins and S. Gambarotta, *Inorg. Synth.*, 1998, **32**, 123.
46 E. Juaristi, P. Murer and D. Seebach, *Synthesis*, 1993, 1243.
47 F. Sorm and L. Sedivy, *Collect. Czech. Chem. Commun.*, 1948, **13**, 289.
48 M. R. Bryce, J. G. Eaves, D. Parker, J. A. K. Howard and O. Johnson, *J. Chem. Soc., Perkin Trans. 2*, 1985, 433.
49 K. Winterfeld and K. Flick, *Arch. Pharm.*, 1956, **289**, 448.
50 D. T. Sawyer, A. Sobkowiak and T. Matsushita, *Acc. Chem. Res.*, 1996, **29**, 409.
51 S. Goldstein and D. Meyerstein, *Acc. Chem. Res.*, 1999, **32**, 547.
52 E. Neyens and J. Baeyens, *J. Hazard. Mater.*, 2003, **98**, 33.
53 L. Zs-Nagy and R. A. Floyd, *Biochim. Biophys. Acta*, 1984, **790**, 238.
54 E. R. Stadtman and B. S. Berlett, *J. Biol. Chem.*, 1991, **266**, 17201.
55 *Bruker, SADABS*, Bruker AXS Inc, Madison, Wisconsin, USA, 2001.
56 G. M. Sheldrick, *Acta Crystallogr., Sect. A: Fundam. Crystallogr.*, 2008, **A64**, 112.